SILICOFCM

Project Title: *In Silico* trials for drug tracing the effects of sarcomeric protein mutations leading to familial cardiomyopathy

Project acronym: SILICOFCM

Grant Agreement number: 777204

Coordinating Institution:
Bioengineering Research and Development Center BioIRC doo Kragujevac, BIOIRC

Start date: 1st June 2018

Duration: 42 months

WP number, Deliverable number and Title	**WP2** Protein and cell data, Imaging processing **D2.3** Imaging Acquisition Data
Related Task	**Task 2.3** Imaging acquisition data
Lead Beneficiary	UNEW
Deliverable Type	Report
Distribution Level	Public
Document version	v.1.0
Contractual Date of Delivery	31/05/2019
Actual Date of Delivery	31/05/2019

Authors	Djordje Jakovljevic (UNEW), Guy MacGowan (UNEW)
Contributors	Nduka Okwose, Amy Fuller, Paul Brennan, Christopher Egget
Reviewers	Lars Maier (UHREG), Iacopo Olivotto (UNIFI), Lazar Velicki (ICVDV)

This project has received funding from the European Union's Horizon 2020 research and innovation programme under grant agreement No 777204

Version history

Version	Description	Date of completion
0.1	Table of contents	01/04/2019
0.2	Finished draft of the document	01/05/2019
0.3	Prefinal version of the document sent to the reviewers	17/05/2019
0.4	Comments & Refinements	25/05/2019
1.0	Final version of the document	31/05/2019

Disclaimer

Executive summary

Noninvasive imaging of the heart is essential to the diagnosis and management of hypertrophic cardiomyopathy (HCM). Echocardiography (i.e. an ultra sound of the heart) is the main technique for screening and characterization of HCM which allows identification of a wide range of structural and functional abnormiality associated with HCM. In addition to and complementing echocardiography, cardiac magnetic resonance imaging (CMRI) has also been used to objectivelay quantify structural and functional abnormalities of the heart in HCM.

HCM was initially suggested to be a disease characterized by hypertrophy of the basal anterior septum and left ventricular outflow obstruction. However, advances in understanding of disease have led to idiscovery of heterogeneous phenotypes within HCM, ranging from minimal to advanced hypertrophy in any location of the left ventricle, subvalvular dysmorphia, presence or absence of outflow tract obstruction, and a range of left ventricular function from hyperdynamic to advancly impaired (end-stage) cardiac dysfunction. Advances in noninvasive imaging including echocardiography and CMRI allow identification and understanding of variety of morphological and functional manifestations in HCM, further advancing management strategies.

This report provides description of imaging techniques used in evaluation, diagnosis, monitoring and management of HCM which will be applied in the prospective clinicla study of the SILICOFCM project.

Table of Contents

List of Figures

List of Abbreviations

Abbreviation	Explanation
ATP	Adenosine Triphosphate
CMRI	Cardiac Magnetic Resonance Imaging
CSI	Chemical Shift Imaging
DPG	2,3, diphosphoglycerate
ECH	Electrocardiogram
EF	Ejection Fraction
HCM	Hypertrophic Cardiomyopathy
IVST	Inter-ventricular Septal Thickness
LADs	Left Atrial End-systolic Diameter
LGE	Late Gadolinium Enhancement
LV	Left Ventricular
LVDd	Left Ventricular End-diastolic Diameter
LVDs	Left Ventricular End-systolic Diameter
LVEDV	Left Ventricular End Diastolic Volume
LVESV	Left Ventricular End Systolic Volume
LVH	Left Ventricular Hypertrophy
LVOT	Left Ventricular Outflow Tract
LVPWT	Left Ventricular Posterior Wall Thickness
LVSV	Left Ventricular Stroke Volume
MRI	Magnetic Resonance Imaging
MV	Mitral Valve
PC-CMR	Phase Control Cardiac Magnetic Resonance
RV	Right Ventricle
SSFP	Steady State Free Precision
STE	Speckle Tracking Echocardiography
TDI	Tissue Doppler Imaging
TTE	Trans-Thoracic Echocardiography
3DE	Three Dimensional Echocardiography

1. Introduction

Hypertrophic cardiomyopathy (HCM) is the most common genetic heart disease with great diversity in phenotypic expression making diagnosis a challenge [1]. HCM affects approximately one in 500 people although rising prevalence has been reported [2]. As a result, HCM currently receives considerable attention mainly because of an associated risk of sudden cardiac death, even in apparently healthy individuals without a prior history of heart disease [3]. The diagnosis of HCM is usually by exclusion thus secondary causes of left ventricular hypertrophy such as systemic hypertension, valvular and subvalvular aortic stenosis, and infiltrative cardiomyopathies has to be ruled out [4].

This report highlights clinical assessment procedures used in the diagnosis and monitoring of HCM with focus on non-invasive imaging techniques, which represent the gold standard. Echocardiography and Cardiac Magnetic Resonance Imaging (CMRI) imaging are detailed in this report with emphasis on structural and functional assessments using these techniques in HCM.

2. Echocardiography

Transthoracic echocardiography is the main form of imaging technique used in HCM. However, transesophageal echocardiogram should be considered in patients with poor transthoracic echo windows, as an alternative or complementary investigation to CMRI [5]. It is particularly useful in patients with left ventricular outflow tract (LVOT) obstruction if the mechanism of obstruction is unclear, when assessing the mitral valve morphology before a septal reduction procedure, and when severe mitral regurgitation caused by intrinsic valve abnormalities is suspected [6]. Contrast-enhanced echocardiography, which involves the use of a contrast agent (e.g. perfluoropropane, sulphur hexafluoride) injected into an upper limb vein, is also used to increase visibility of the heart. Echocardiography assessment is important to demonstrate severity and distribution of left ventricular hypertrophy, further showing structural and functional characteristics of mitral valves and subvalvular apparatus, assess left ventricular outflow tract obstruction and evaluate diastolic dysfunction. Sections 2.2 and 2.3 provide more details on imaging modalities used in evaluation of HCM.

2.1 Echocardiography Imaging Techniques

Several echocardiography techniques have been used in HCM. Apical or anterolateral wall hypertrophy could be easily missed and the use of contrast agents for cavity opacification is vital, just like for the detection of apical aneurysms and thrombus [7,8]. Three-dimensional echocardiography (3DE) has been purported to be more accurate in mass quantification however evidence supporting routine clinical use remains limited [7]. Strain rate imaging obtained by Tissue Doppler Imaging (TDI) and Speckle Tracking Echocardiography (STE) is a useful tool to differentiate HCM from hypertensive cardiomyopathy as more remarkable reductions in strains are demonstrated in HCM compared to the latter [9]. Longitudinal strain analysis by STE enables early detection of left ventricular (LV) contraction abnormalities in patients with preserved ejection fraction [10]. Apical and Septal HCM have common LV contraction pattern; longitudinal strain is lower, circumferential strain is higher and twist is apically displaced [11].

2.2 Echocardiography Assessments of Cardiac Structure in HCM

2.2.1 Left Ventricular Hypertrophy

The most common region for increased left ventricular wall thickness is the anterior septum although hypertrophy can involve any region of the myocardium [12]. Increased septal thickness could be global occurring throughout the septum, basal or apical (Figure 1). A progressive increase in the risk of sudden cardiac death is associated with increasing wall thickness, with a cut-off of ≥30 mm representing “massive” hypertrophy [13]. While the anterior portion of the septum is more commonly involved in HCM, hypertrophy could be observed at the posterior septum in some patients. Furthermore, HCM may be encountered at the anterior free wall, lateral wall and rarely the posterior wall of the left ventricle.

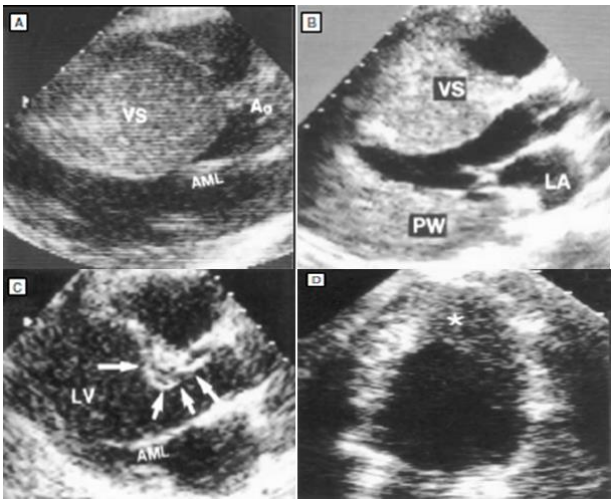

Figure 1. Heterogeneity of pattern and extent of septal hypertrophy in HCM. Echocardiographic parasternal long axis stop frame images obtained in diastole showing A, massive asymmetric hypertrophy of ventricular septum (VS); B, Pattern of septal hypertrophy showing considerable apical and mid-septal hypertrophy compared to the basal septum; C, hypertrophy confined to basal septum just below the aortic valve (arrows); D, hypertrophy confined to LV apex (asterisk), consistent with the designation of apical hypertrophic cardiomyopathy. Adapted from [14].

2.2.2 Mitral Valve and Subvalvular Abnormalities

A number of morphological abnormalities involving the mitral valve (MV) and subvalvular structures are part of the phenotypic expression of HCM [15]. A vast majority of patients with HCM have substantially elongated mitral leaflets (Figure 2) compared to controls irrespective of LV wall thickness or mass index [16], most commonly involving the anterior leaflet but the posterior or both leaflets can also be involved [12]. Elongated MV leaflets sometimes exhibit systolic anterior motion and contribute to left ventricular outflow tract (LVOT) obstruction by making more distal contact with the septum than usually seen [12].

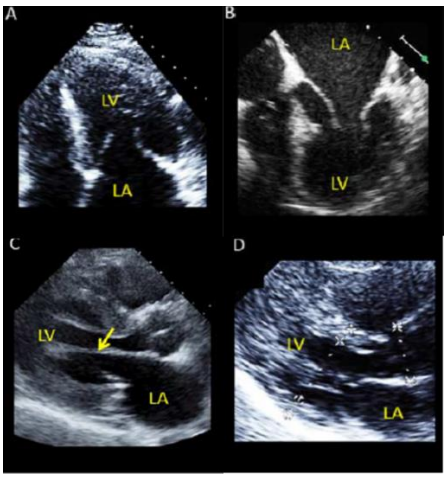

Figure 2. Abnormalities of the mitral valve in HCM Patients; A and B showing elongated mitral valve leaflets; C and D showing long mitral valve leaflets contributing to obstruction despite minimal septal hypertrophy. Adapted from [12].

Numerous papillary muscle abnormalities have also been described in HCM [17]. HCM patients often have an increased number of papillary muscles, which are often hypertrophied and apically orientated towards the ventricular septum [18]. For this reason, these abnormally displaced papillary muscles often contribute to outflow obstruction by pulling the plane of the MV toward the septum. LV apical–basal muscle bands have also been described in HCM and often have abnormal chordal connections to the MV, which further contribute to the mechanism of LVOT obstruction [12] (Figure 3). The LV cavity is generally normal or small in size with a hyperdynamic ventricle and a high ejection fraction. Most patients may live without symptoms for many decades. The right ventricular (RV) wall thickness and mass are increased in one-third of HCM patients, predominantly as a diffuse process involving the entire or a significant proportion of the RV wall [19].

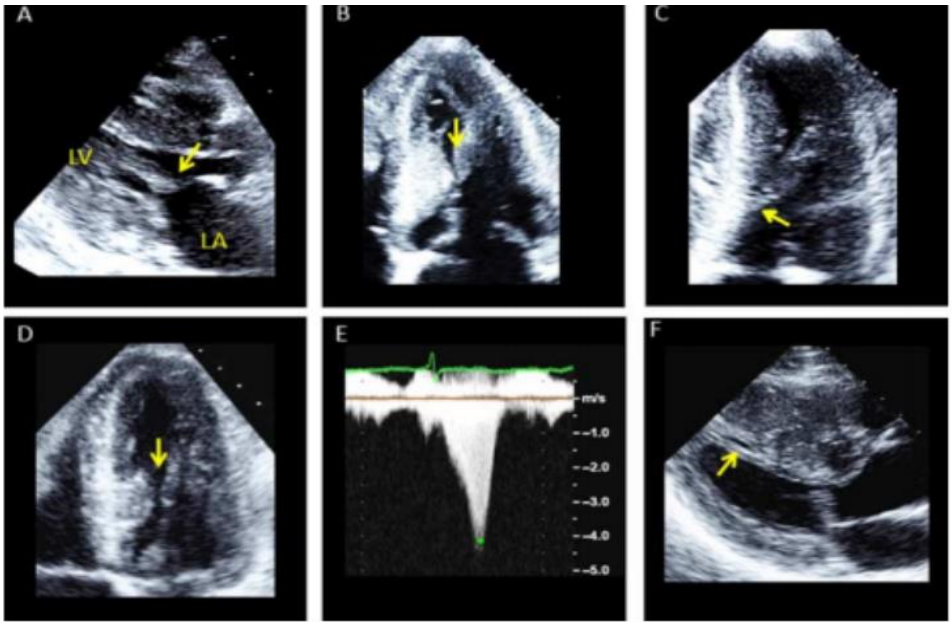

Figure 3. Spectrum of subvalvular abnormalities in HCM; A, Direct attachment of anterior papillary muscle to anterior MV leaflet (yellow arrow); B, Hypertrophied papillary muscle narrowing the LVOT; C, D and E, Anteriorly oriented papillary muscle encroaching on the LVOT (arrows) and contributing to outflow gradient; F, Abnormal muscle band with attachment to the septum (arrow). Adapted from [12].

2.2.3 Left Ventricular Outflow Tract Obstruction

Left Ventricular Outflow Tract Obstruction (LVOT) obstruction is an independent predictor of prognosis in HCM patients [12]. It is also implicated as a major factor contributing to symptoms such as dyspnea, chest pain and syncope [1,20]. Therefore, it is vital to assess LVOT gradient in these patients. One-third of patients with HCM exhibit gradients ≥30 mmHg at rest. Provocations such as using Valsalva manoeuvre, amyl nitrite inhalation, premature ventricular contraction, infusion of dobutamine or isoproterenol, and exercise (Figure 4) can provoke latent obstruction in another one-third of patients [12]. Thus, the majority of HCM patients exhibit resistance to left ventricular outflow either at rest or with physiological or pharmacological challenge.

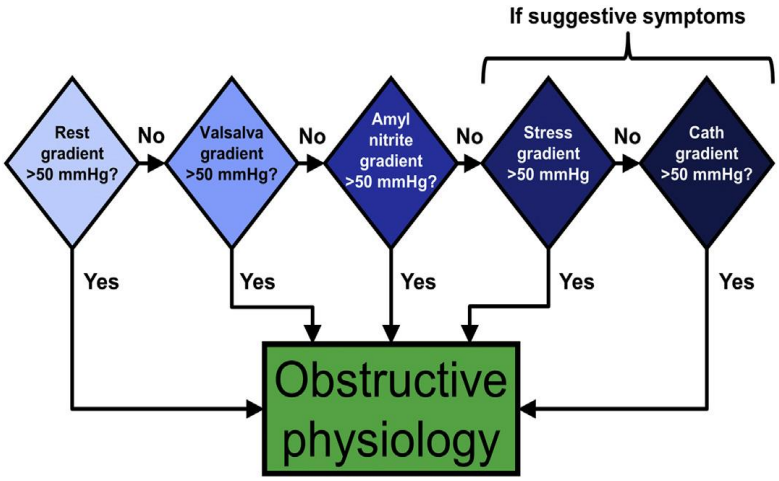

Figure 4. Stepwise approach to defining Obstructive Physiology in HCM. Although a gradient of 30 mm Hg constitutes the presence of obstruction, a gradient of 50 mm Hg (severe obstruction) is used as the cut-off for this decision-making algorithm. If a gradient of 50 mm Hg is not present at rest, a Valsalva manoeuvre is performed. Adapted from [4].

The Valsalva is the simplest echocardiographic examination among all provocative manoeuvres and could be easily performed at bedside. However, exercise is the preferable method because it is the closest to representing the conditions of real life that result in symptoms in patients during daily activities (Figure 5). An LVOT gradient of ≥50 mmHg at rest or with provocation is the cut-off necessary for recommending invasive septal reduction therapy [5].

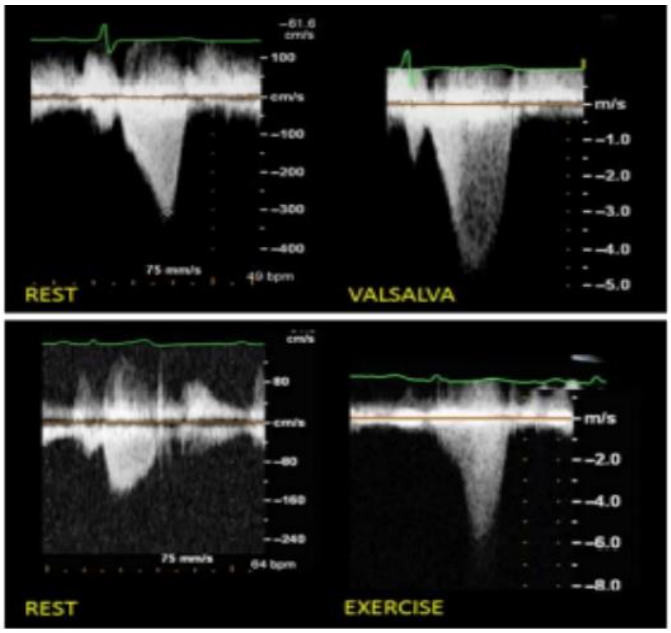

Figure 5. Doppler recordings of LVOT gradients from two patients with HCM. Top panel shows only a mild gradient at rest in a HCM patient, increasing significantly with Valsalva manoeuver; bottom panel depicts LVOT velocity in a patient, which increases markedly with exercise. Adapted from [12].

2.3 Echocardiography Assessments of Cardiac Function in HCM

2.3.1 Assessment of Diastolic Function

Patients with HCM often present with diastolic dysfunction with left atrial dilatation being one of the most common morphologic evidence [21]. Assessment of LV filling pressures is helpful in the evaluation of symptoms and disease progression. Doppler echocardiographic parameters are sensitive measures of diastolic function, but are influenced by loading conditions, heart rate and age, thus, there is no single echocardiographic parameter that can be used as a diagnostic hallmark of LV diastolic dysfunction [22]. Therefore, a comprehensive evaluation of diastolic function which includes; Doppler myocardial imaging, pulmonary vein flow velocities, pulmonary artery systolic pressure and left atrial size is recommended as part of the routine assessment of HCM [22]. Patients with a restrictive left ventricular filling pattern (ratio of mitral peak velocity of early filling [E] to mitral peak velocity of late filling [A] ≥2; and E-wave deceleration time ≤150 ms) may be at higher risk for adverse outcome, even with a preserved ejection fraction (EF) [23, 24].

2.3.2 Assessment of Systolic Function

Radial contractile function (ejection fraction (EF) or fractional shortening) is typically normal or increased in patients with HCM. However, EF is a poor measure of LV systolic performance when hypertrophy is present [25]. Longitudinal velocities and markers of deformation (strain and strain rate), derived from Doppler myocardial imaging or speckle tracking techniques, are usually reduced in HCM patients despite a normal EF [5]. Myocardial longitudinal deformation is typically reduced at the site of hypertrophy [11].

The above described echocardiography procedures will be used in the clinical prospective study of the SILICOFCM project. Additional measurements that will also be performed using TTE include; LV end-diastolic volume (LVEDV), LV end-systolic volume (LVESV), LV stroke volume (LVSV), LV end-diastolic diameter (LVDd), LV end-systolic diameter (LVDs), LV posterior wall thickness (LVPWT), inter-ventricular septal thickness (IVST), and left atrial end-systolic dimension (LADs).

3. Cardiac Magnetic Resonance Imaging

Assessment of cardiomyopathies with cardiac magnetic resonance imaging (CMRI) has been successful considering its unique ability to characterize different patterns in diseased myocardium and increased accuracy (sensitivity and specificity) compared to transthoracic echocardiography [26]. CMRI has become an established method for evaluation of HCM due to unrestricted view of the entire myocardium, more accurate measurement of LV wall thickness, mass, volumes and function and its ability to provide non-invasive assessment of myocardial fibrosis [27].

3.1 Cardiac Magnetic Resonance Imaging Techniques in HCM

Cine steady state free precision (SSFP) magnetic resonance imaging is used for morphological assessment of HCM and cardiac function measurement because of the high contrast between the myocardium and blood and high temporal resolution [28]. Steady-state free precession is able to define all phenotypes of HCM as there is no restriction to the view of the myocardium. Apical hypertrophic cardiomyopathy or localized myocardial hypertrophy (e.g. inferior septum or lateral wall), which can be missed by echocardiography, is easily identified with SSFP. Cine SSFP shows not only the wall motion but also the turbulence jet across the LVOT in patients with asymmetrical septal hypertrophy [29]. Late gadolinium enhancement is the most valuable CMRI technique as it precisely identifies myocardial replacement fibrosis or scarring that contributes to risk stratification in HCM [29]. Other CMRI techniques include; Cine phase contrast MR imaging, used to quantify the blood flow passing through the LVOT; Cardiac tagging for evaluating the myocardial wall motion and strain,; Perfusion imaging, which provides information about blood flow and myocardial circulation with high spatial and temporal resolution and T_1 and T_2 mapping imaging techniques are able to identify myocardial injuries associated with HCM without gadolinium-based contrast agents [29].

Clinical partners within the SILICOFCM will perform CMRI in eligible patients participating in the prospective study. The CMRI techniques which will be used include cine imaging, cardiac spectroscopy, cardiac tagging and late gadolinium enhancement. A 3-Tesla Intera Achieva scanner (Philips, Best, NL) will be used for assessments and more details on the respective scanning techniques are provided in the subsequent sections.

3.1.1 Cine Imaging

Subjects will be scanned in supine position using a 6- channel cardiac coil and ECG gating (Philips). short-axis balanced SSFP images covering the entire left ventricle [field of view (FOV) 350 × 350 mm2, repetition time/echo time (TR/TE) = 3.7/ 1.9 ms, turbo factor 17, flip angle (FA) 40°, slice thickness 8 mm, 25 phases, resolution 1.37 mm] will be obtained [30]; long-axis images will also be acquired. Endocardial and epicardial borders will be traced manually on short-axis slices throughout the cardiac cycle using the View Forum workstation (Philips). LV mass, and systolic and diastolic parameters, including the ratio of early to late ventricular filling velocity (E/A ratio) and early filling percentage, will be calculated using previously described methods [31]. Longitudinal shortening will be determined in the four-chamber view as the percentage difference in distance from the mitral valve plane to the apex at end-systole and end-diastole. The myocardial wall thickness will be determined at the same level as

tagging, and the percentage increase from diastole to systole (radial thickening) will be calculated. Cine phase contrast image is shown in Figure 6.

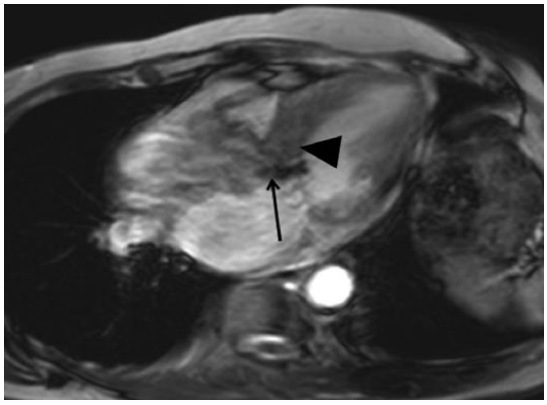

Figure 6. Cine phase contrast image. Cine steady-state free precession (SSFP) shows not only high septal myocardial hypertrophy (arrowhead) but also turbulence jet across the left ventricular outflow tract (arrow). Adapted from [29].

3.1.2 Cardiac Spectroscopy

Subjects were scanned prone, using a 10-cm diameter ^{31}P surface coil (Pulseteq, UK). A cardiac gated one-dimensional (1-D) chemical shift imaging (CSI) sequence will be used with spatial pre-saturation of the skeletal muscle. A 7-cm slice using a 'spredrex'-type pulse of 2.3 ms duration will be selected to eliminate liver contamination. Negligible liver contamination will be ensured with 1-D foot-head oriented CSI experiments in phantoms: <1% of the total phosphorus signal originated from outside the prescribed volume. Sixteen coronal phase-encoding steps would yield spectra from 10-mm slices (TR = heart rate, 192 averages, acquisition time approximately 20 min). The first spectrum arising entirely beyond the chest wall will be analysed using the AMARES time domain fit [32] to quantify PCr, the gamma resonance of adenosine triphosphate (ATP), and 2,3-diphosphoglycerate (DPG). The ATP peak area will be corrected for blood contamination by 1/6th combined 2,3-DPG peak, and PCr/ATP ratios will be corrected for T1 saturation and local flip angle [31]. ^{31}P magnetic resonance spectroscopy is shown in Figure 7.

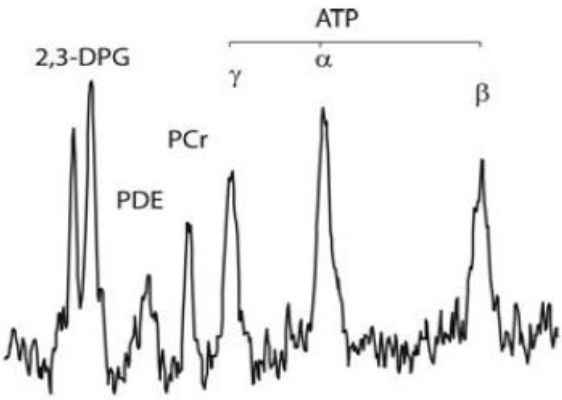

Figure 7. ^{31}P magnetic resonance spectroscopy. Representative spectra from a patient with Phosphocreatine to adenosine triphosphate (PCr/ATP) ratio of 1.23. Adapted from [33].

3.1.3 Cardiac Tagging

Magnetic resonance signal from the myocardium in diastole will be cancelled in a rectangular grid pattern and tags tracked through the cardiac cycle (Figure 8A) [30]. A multi-shot turbo-field echo sequence will be used (TR/TE/FA/number of averages = 4.9/3.1/10°/1, turbo factor 9, SENSE factor 2, FOV 350 × 350 mm2, voxel size 1.37 mm, tag spacing 7 mm, 12 phases). Two adjacent short-axis slices of 10 mm thickness will be acquired at the mid-ventricle with a 2-mm gap. The Cardiac Image Modeling package (Auckland UniServices Ltd, Auckland, New Zealand) will be used to align a mesh on the tags between the endocardial and epicardial contours. Peak circumferential strain for both the whole myocardial wall and the endocardial third will also be calculated. Peak torsion between the two slices will be calculated as the circumferential-longitudinal shear angle, defined on the epicardial surface (Figure 8B) [34].

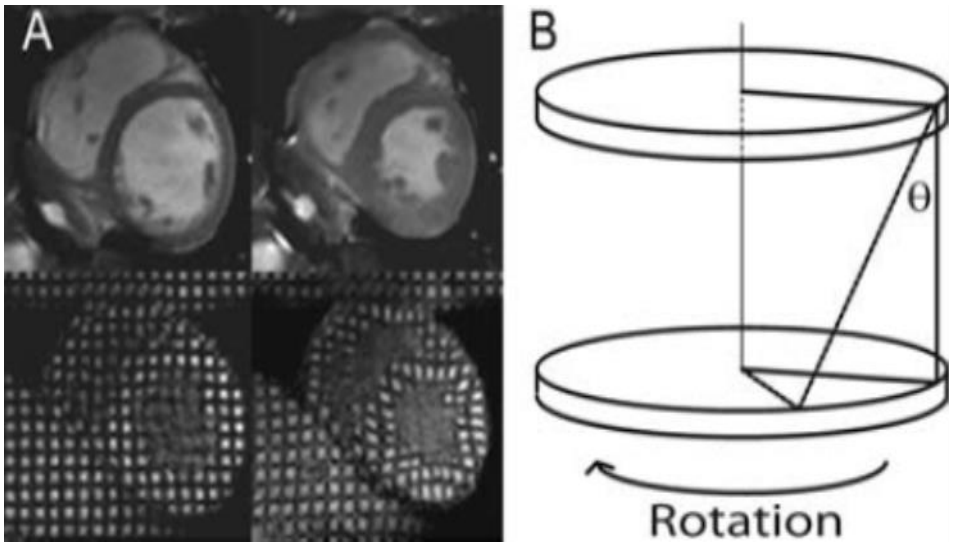

Figure 8. Cardiac tagging analysis. (A) Cine imaging (top panels) and tagging (bottom) at end-diastole (left panels) and end-systole (right). A rectangular grid of nulled myocardium applied in the diastole enables tracking of myocardial deformation. (B) Tagging of two parallel short-axis slices allows the calculation of torsion, the longitudinal-circumferential sheer angle (u) as shown. Adapted from [33].

3.1.4 Late Gadolinium Enhancement

Where indicated, Gadolinium-DTPA of 0.2 mmol/kg (Dotarem, Guerbet, France) will be administered intravenously to patients. LGE images will be obtained at 10 min using a breath-held, cardiac-triggered three-dimensional phase-sensitive inversion recovery sequence (multi-shot gradient echo TR/TE = 5/2.4, FA = 15°/5°, acceleration factor 31, parallel imaging factor 2, 1.8-mm resolution zero-filled to 1.3 mm) with the inversion time to null normal myocardium determined from a prior multi-slice 2D Look-Locker experiment (multi-shot EPI with an EPI factor 5, acceleration factor 2, TR/TE = 7.3/2.8, 3-mm resolution) [30]. Qualitative analysis for the presence and distribution of LGE in a 17-segment model will be performed by two experienced, independent observers, blinded to patient status and MRI/MRS findings as per Society for Cardiovascular Magnetic Resonance guidelines [35]. Figure 9 shows late gadolinium enhancement and associated intraventricular thrombus observed in mid-ventricular obstruction HCM.

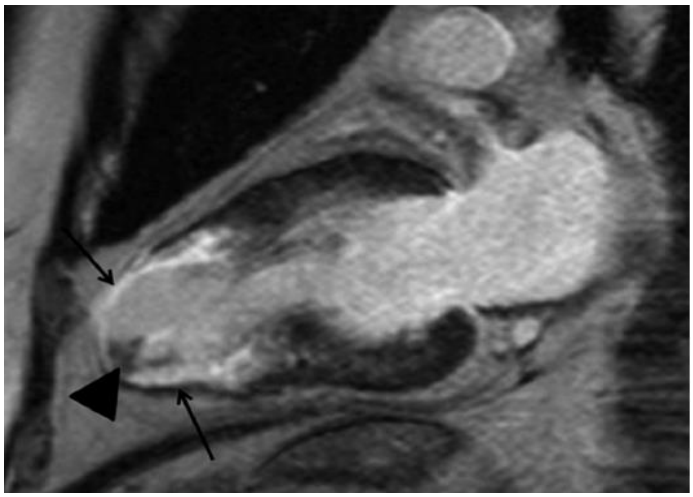

Figure 9. Apical Aneurysm showing late gadolinium enhancement (arrows) and associated intraventricular thrombus (arrowhead) observed in mid-ventricular obstruction HCM. Adapted from [29].

3.2 CMRI Assessment of Cardiac Structure and Function in HCM

In patients with good echocardiographic images, CMRI provides similar information on ventricular function and morphology [36]. CMRI is superior to transthoracic echocardiography (TTE) in the measurement of LV mass [36] and LV apical and anterolateral hypertrophy and aneurysms [37]. It is also more sensitive in the detection of elusive markers of disease, such as myocardial crypts and papillary muscle abnormalities in patients with sarcomeric protein gene mutations [38, 39]. Phase velocity flow mapping sequences can be used to determine the peak velocity of blood flow through the LV outflow tract in patients with LVOT obstruction however, loss of signal due to phase offset errors could make the accurate quantification of flow difficult during stress thus making Doppler echocardiography the modality of choice for quantification of LVOT obstruction. Similarly, while mitral inflow velocities and pulmonary vein flow derived from phase contrast CMR (PC-CMR) provide highly reproducible and accurate data, echocardiography is the preferred method for assessment of diastolic function in routine practice. By using the intrinsic magnetic properties of different tissues and the distribution of gadolinium-based contrast agents, CMRI could be used to detect expansion of the myocardial interstitium caused by fibrosis. Late gadolinium enhancement (LGE) is present typically in a patchy mid-wall pattern in areas of hypertrophy and at the anterior and posterior right ventricular insertion points [40]. LGE is unusual in non-hypertrophied segments except in advanced stages of disease, when full-thickness LGE in association with wall thinning is common [40]. LGE may be associated with increased myocardial stiffness and adverse LV remodelling and the extent of LGE is associated with a higher incidence of regional wall motion abnormalities. Late gadolinium enhancement varies substantially with the quantification method used and the 2-standard deviation technique is the only one validated against necropsy.

4. Deviation from work Plan

No deviation from work plan recorded.

5. Conclusion

Noninvasive imaging techniques are crucial in diagnosis and management of HCM. Echocardiography is a standard clinical tool for screening for the disease and characterization of HCM phenotype and can identify a wide array of abnormalities in myocardial structure and function. CMRI provides high-fidelity in-depth morphologic information such as myocardial fibrosis depending on the presence and extent of LGE thus enhancing prognostic accuracy. SILICOFCM clinical prospective study will use both echocardiography and CMRI to evaluate disease progression and response to pharmacological and lifestyle intervention in HCM.

6. References

[1] Maron BJ, Ommen SR, Semsarian C, Spirito P, Olivotto I, Maron MS. Hypertrophic cardiomyopathy: present and future, with translation into contemporary cardiovascular medicine. Journal of the American College of Cardiology (2014); 64(1): pp. 83-99.

[2] Semsarian C, Ingles J, Maron MS, Maron BJ. New perspectives on the prevalence of hypertrophic cardiomyopathy. Journal of the American College of Cardiology (2015); 65(12): pp. 1249-1254.

[3] Christiaans I, Elliott PM. Hypertrophic cardiomyopathy. In: Clinical Cardiogenetics (2nd ed.), 2016.

[4] Geske JB, Ommen SR, Gersh BJ. Hypertrophic Cardiomyopathy: Clinical Update. Journal of the American College of Cardiology: Heart Failure (2018); 6(5): pp. 364-375.

[5] Zamorano JL, Anastasakis A, Borger MA, Borggrefe M, Cecchi F, Charron P, et al. 2014 ESC guidelines on diagnosis and management of hypertrophic cardiomyopathy: The task force for the diagnosis and management of hypertrophic cardiomyopathy of the European Society of Cardiology (ESC). European Heart Journal (2014); 35(39): pp. 2733–2779.

[6] Oki T, Fukuda N, Iuchi A, Tabata T, Tanimoto M, Manabe K, et al. Transesophageal echocardiographic evaluation of mitral regurgitation in hypertrophic cardiomyopathy: Contributions of eccentric left ventricular hypertrophy and related abnormalities of the mitral complex. Journal of the American Society of Echocardiography (1995); 8(4): pp. 503-510.

[7] Nagueh SF, Bierig SM, Budoff MJ, Desai M, Dilsizian V, Eidem B, et al. American society of echocardiography clinical recommendations for multimodality cardiovascular imaging of patients with hypertrophic cardiomyopathy: Endorsed by the American society of nuclear cardiology, society for cardiovascular magnetic resonance, and society of cardiovascular computed tomography. Journal of the American Society of Echocardiography (2011); 24(5): pp. 473-498.

[8] Parato VM, Olivotto I, Maron MS, Nanda NC, Pandian NG. Left Ventricular Apex Involvement in Hypertrophic Cardiomyopathy. Echocardiography (2015); 32(10): pp. 1575–1580.

[9] Kato TS, Noda A, Izawa H, Yamada A, Obata K, Nagata K, et al. Discrimination of nonobstructive hypertrophic cardiomyopathy from hypertensive left ventricular hypertrophy on the basis of strain rate imaging by tissue Doppler ultrasonography. Circulation (2004); 110(25): pp. 3808-3814.

[10] Parato VM, Antoncecchi V, Sozzi F, Marazia S, Zito A, Maiello M, et al. Echocardiographic diagnosis of the different phenotypes of hypertrophic cardiomyopathy. Cardiovascular Ultrasound (2015); 14(1): pp. 30.

[11] Yang H, Carasso S, Woo A, Jamorski M, Nikonova A, Wigle ED, et al. Hypertrophy pattern and regional myocardial mechanics are related in septal and apical hypertrophic cardiomyopathy Journal of the American Society of Echocardiography (2010); 23(10): pp. 1081–1089.

[12] Pandian NG, Rowin EJ, Gonzalez AMG, Maron MS. Echocardiographic profiles in hypertrophic cardiomyopathy: imaging beyond the septum and systolic anterior motion. Echo Research and Practice (2015); 2(1): E1-7.

[13] Ong KC, Geske JB, Hebl VB, Nishimura RA, Schaff H V., Ackerman MJ, et al. Pulmonary hypertension is associated with worse survival in hypertrophic cardiomyopathy. European Heart Journal - Cardiovascular Imaging (2016); 17(6): pp. 604-610.

[14] Maron BJ. Hypertrophic cardiomyopathy: a systematic review. Journal of the American Medical Association (2002); 287(10): pp. 1308 – 1320.

[15] Kaple RK, Murphy RT, DiPaola LM, Houghtaling PL, Lever HM, Lytle BW, et al. Mitral Valve Abnormalities in Hypertrophic Cardiomyopathy: Echocardiographic Features and Surgical Outcomes. The Annals of Thoracic Surgery (2008); 85(5): pp. 1527-1535.

[16] O'Hanlon R, Grasso A, Roughton M, Moon JC, Clark S, Wage R, et al. Prognostic significance of myocardial fibrosis in hypertrophic cardiomyopathy. Journal of the American College of Cardiology (2010); 56(11): pp. 867-874.

[17] Austin BA, Kwon DH, Smedira NG, Thamilarasan M, Lever HM, Desai MY. Abnormally Thickened Papillary Muscle Resulting in Dynamic Left Ventricular Outflow Tract Obstruction: An Unusual Presentation of Hypertrophic Cardiomyopathy. Journal of the American Society of Echocardiography (2009); 22(1): 105.e5-6.

[18] Chan RH, Maron BJ, Olivotto I, Pencina MJ, Assenza GE, Haas T, et al. Prognostic value of quantitative contrast-enhanced cardiovascular magnetic resonance for the evaluation of sudden death risk in patients with hypertrophic cardiomyopathy. Circulation (2014); 130(6): pp. 484-495.

[19] Malik R, Maron MS, Rastegar H, Pandian NG. Hypertrophic cardiomyopathy with right ventricular outflow tract and left ventricular intracavitary obstruction. Echocardiography (2014); 31(5): pp. 682–685.

[20] Williams LK, Gruner CH, Rakowski H. The Role of Echocardiography in Hypertrophic Cardiomyopathy. Current Cardiology Reports (2015); 17(2): pp. 6.

[21] Douglas PS. The left atrium: a biomarker of chronic diastolic dysfunction and cardiovascular disease risk. Journal of the American College of Cardiology (2003); 42(7): pp. 1206–1207.

[22] Nagueh SF, Appleton CP, Gillebert TC, Marino PN, Oh JK, Smiseth OA, et al. Recommendations for the evaluation of left ventricular diastolic function by echocardiography. European Journal of Echocardiography (2009); 29(4): pp. 277-314.

[23] Kubo T, Gimeno JR, Bahl A, Steffensen U, Steffensen M, Osman E, et al. Prevalence, clinical significance, and genetic basis of hypertrophic cardiomyopathy with restrictive phenotype. Journal of the American College of Cardiology (2007); 49(25): pp. 2419–2426.

[24] Biagini E, Spirito P, Rocchi G, Ferlito M, Rosmini S, Lai F, et al. Prognostic Implications of the Doppler Restrictive Filling Pattern in Hypertrophic Cardiomyopathy. The American Journal of Cardiology (2009); 104(12): pp. 1727–1731.

[25] Maciver DH. A new method for quantification of left ventricular systolic function using a corrected ejection fraction. European Journal of Echocardiography (2011); 12(3): pp. 228–234.

[26] Moon JCC, Fisher NG, McKenna WJ, Pennell DJ. Detection of apical hypertrophic cardiomyopathy by cardiovascular magnetic resonance in patients with non-diagnostic echocardiography. Heart (2004); 90(6): pp. 645–649.

[27] Hoey ETD, Elassaly M, Ganeshan A, Watkin RW, Simpson H. The role of magnetic resonance imaging in hypertrophic cardiomyopathy. Quantitative Imaging in Medicine and Surgery (2014); 4(5): pp. 397.

[28] Carr JC, Simonetti O, Bundy J, Li D, Pereles S, Finn JP. Cine MR Angiography of the Heart with Segmented True Fast Imaging with Steady-State Precession. Radiology (2001); 219(3): pp. 828–834.

[29] Amano Y, Kitamura M, Takano H, Yanagisawa F, Tachi M, Suzuki Y, et al. Cardiac MR Imaging of Hypertrophic Cardiomyopathy: Techniques, Findings, and Clinical Relevance. Magnetic Resonance

in Medical Sciences (2018);17(2): pp. 120–131.

[30] Bates MGD, Hollingsworth KG, Newman JH, Jakovljevic DG, Blamire AM, MacGowan GA, et al. Concentric hypertrophic remodelling and subendocardial dysfunction in mitochondrial DNA point mutation carriers. European Heart Journal - Cardiovascular Imaging (2013); 14(7): pp. 650-658.

[31] Jones DEJ, Hollingsworth K, Fattakhova G, MacGowan G, Taylor R, Blamire A, et al. Impaired cardiovascular function in primary biliary cirrhosis. American Journal of Physiology - Gastrointestinal and Liver Physiology (2010); 298(5): G764-773.

[32] Vanhamme L, Van Huffel S, Van Hecke P, van Ormondt D. Time-Domain Quantification of Series of Biomedical Magnetic Resonance Spectroscopy Signals. Journal of Magnetic Resonance (1999); 140(1): pp. 120–130.

[33] Bates MGD, Hollingsworth KG, Newman JH, Jakovljevic DG, Blamire AM, MacGowan GA, et al. Concentric hypertrophic remodelling and subendocardial dysfunction in mitochondrial DNA point mutation carriers. European Heart Journal - Cardiovascular Imaging (2013); 14(7): pp. 650–658.

[34] Lumens J, Delhaas T, Arts T, Cowan BR, Young AA. Impaired subendocardial contractile myofiber function in asymptomatic aged humans, as detected using MRI. American Journal of Physiology-Heart and Circulatory Physiology (2006); 291(4): H1573–1579.

[35] Hundley WG, Bluemke D, Bogaert JG, Friedrich MG, Higgins CB, Lawson MA, et al. Society for Cardiovascular Magnetic Resonance guidelines for reporting cardiovascular magnetic resonance examinations. Journal of Cardiovascular Magnetic Resonance (2009); 11(1): pp. 5.

[36] Olivotto I, Maron MS, Autore C, Lesser JR, Rega L, Casolo G, et al. Assessment and Significance of Left Ventricular Mass by Cardiovascular Magnetic Resonance in Hypertrophic Cardiomyopathy. Journal of the American College of Cardiology (2008); 52(7): pp. 559–566.

[37] Maron MS, Finley JJ, Bos JM, Hauser TH, Manning WJ, Haas TS, et al. Prevalence, Clinical Significance, and Natural History of Left Ventricular Apical Aneurysms in Hypertrophic Cardiomyopathy. Circulation (2008); 118(15): pp. 1541–1549.

[38] Germans T, Wilde AAM, Dijkmans PA, Chai W, Kamp O, Pinto YM, et al. Structural Abnormalities of the Inferoseptal Left Ventricular Wall Detected by Cardiac Magnetic Resonance Imaging in Carriers of Hypertrophic Cardiomyopathy Mutations. Journal of the American College of Cardiology (2006); 48(12): pp. 2518–2523.

[39] Maron MS, Rowin EJ, Lin D, Appelbaum E, Chan RH, Gibson CM, et al. Prevalence and Clinical Profile of Myocardial Crypts in Hypertrophic Cardiomyopathy. Circulation: Cardiovascular Imaging (2012); 5(4): pp. 441–447.

[40] Rudolph A, Abdel-Aty H, Bohl S, Boyé P, Zagrosek A, Dietz R, et al. Noninvasive Detection of Fibrosis Applying Contrast-Enhanced Cardiac Magnetic Resonance in Different Forms of Left Ventricular Hypertrophy. Journal of the American College of Cardiology (2009); 53(3): pp. 284–291.

End of document